Title	Photonic chiplet integration on optical interposer: Can hybrid bonding realize passive optical coupling?
Authors	Hwang, How Yuan;O'Brien, Peter
Publication date	2024-08-09
Original Citation	Hwang, H. Y. and O'Brien, P. (2024) 'Photonic chiplet integration on optical interposer: Can hybrid bonding realize passive optical coupling?', 2024 Photonics & Electromagnetics Research Symposium (PIERS), Chengdu, China, 21-25 April 2024, pp. 1-7. https://doi.org/10.1109/PIERS62282.2024.10618259
Type of publication	Conference item
Link to publisher's version	10.1109/PIERS62282.2024.10618259
Rights	© 2024, IEEE. Personal use of this material is permitted. Permission from IEEE must be obtained for all other uses, in any current or future media, including reprinting/republishing this material for advertising or promotional purposes, creating new collective works, for resale or redistribution to servers or lists, or reuse of any copyrighted component of this work in other works.
Download date	2026-08-08 23:42:17
Item downloaded from	https://hdl.handle.net/10468/16607

Photonic Chiplet Integration on Optical Interposer: Can Hybrid Bonding Realize Passive Optical Coupling?

How Yuan Hwang and Peter O'Brien

Tyndall National Institute, Ireland

Abstract— Silicon photonic integrated circuits (Si-PIC) have come a long way since Soref *et al* first proposed the use of silicon waveguides in the mid-1980s. However, even after four decades, packaging and integration of silicon photonic systems remain an under-studied area. Most of the packaging activities have been focusing on Fibre-to-PIC coupling, and how to achieve the lowest possible coupling loss. In this paper, we look beyond Fibre-to-PIC coupling, and explore the possibility of PIC-to-PIC integration through a 2.5D optical interposer. We opine that hybrid bonding approach could be a suitable technology for passive PIC-to-PIC integration because it is based on A. gapless (oxide fusion bonding), B. bump-less electrical connection (direct Cu-to-Cu) and C. has a relatively high bonding accuracy (~0.5 µm). Two optical coupling approaches were studied – grating-to-grating coupling, and evanescent coupling based on inverted taper pair. FDTD was used in this activity – first to understand the feasibility of the two coupling approaches and then how potential bonding misalignment can affect PIC-to-PIC coupling losses.

1. INTRODUCTION

Silicon photonic integrated circuits (Si-PIC) industries have seen an explosive growth over the last decade with almost all major foundries already releasing their own process and design kits (PDKs), driven by an increasing list of functionalities and applications. However, packaging and integration of Si-PIC systems remain an under-studied area and most activities have been focusing on Fibre-to-PIC coupling, and how to realize the lowest possible coupling loss. While Fibre-to-PIC coupling will continue to be a critical building block, we opine that attention should also be placed on the next stage of photonic system integration, just like the way the electronic industries have evolved over the years. But before that, let us look at the current Si-PIC integration approach.

First, Si-PIC designs typically follow a certain rule of thumb regarding the position of optical interconnects for Fibre-to-PIC coupling. For example, edge couplers must be placed at the edge of the Si-device, while grating couplers have slightly more freedom depending on whether flip-chip or wire bonding integration is used. Due to the position constraint of these optical interconnects, a large area of the Si-PIC must be used to route the optical waveguides. Second, Si-PIC are almost all monolithically integrated, whereby each foundries offer all possible components in their PDKs, except for light emitting components, which must be either externally coupled or heterogeneously integrated onto the Si-PIC.

Food for thought - What if we can place optical interconnects anywhere on the Si-PIC? What if we can choose individual components with the best performance from different foundries and combine them into a photonic system? What if we can passively assemble individual electronic and photonic chiplets onto an interposer to form a system in package? While chiplets approach have been used in the electronics industries for years, it is not straightforward for photonics due to optical coupling requirements. In this paper, we explore the feasibility of coupling between a pair of optical interconnects.

2. CONCEPT AND APPROACH

A schematic of a hybrid bonded Si-PIC to interposer is shown in Fig. 1. We opine that hybrid bonding can be an attractive approach to realize electro-photonic system in package because it is A. gapless (oxide fusion bonding), B. bump-less electrical connection (direct Cu-to-Cu) and C. has a relatively high bonding accuracy (~0.5 µm). The combination of the above would allow potential passive optical coupling between two vertically positioned optical interconnect. In general, hybrid bonding process involves A. room temperature oxide-to-oxide fusion and B. thermal annealing for copper-to-copper bonding. A general process flow of hybrid bonding is shown in Fig. 2. Further information regarding oxide/copper hybrid bonding can be found in [1, 2] while low temperature hybrid bonding approaches can be found in [3, 4]. There are also alternative hybrid bonding approaches that rely on organic bonding layer instead of oxide and can be found in [5-7].

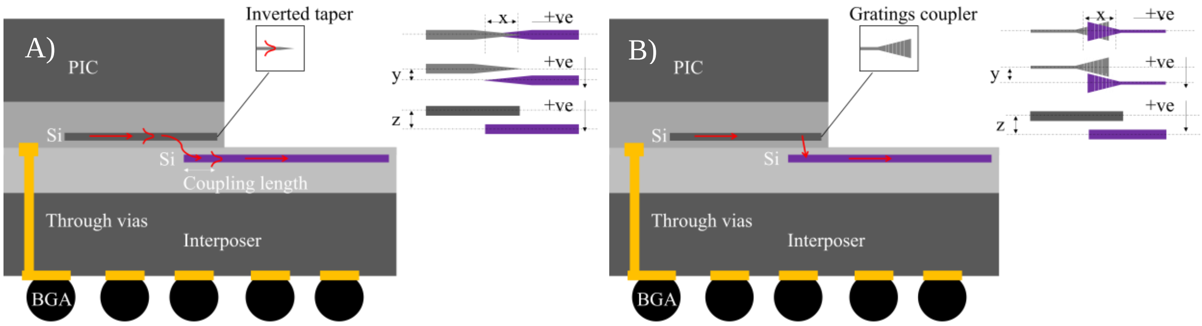

Fig. 1. Schematics of hybrid bonded photonic chiplet of optical interposer. Two optical coupling approaches were shown – A) inverted tapers and B) grating couplers. Relative directions for simulations in the x-, y- and z- positions are defined in the schematics. The materials for optical couplers can be either silicon or silicon nitride.

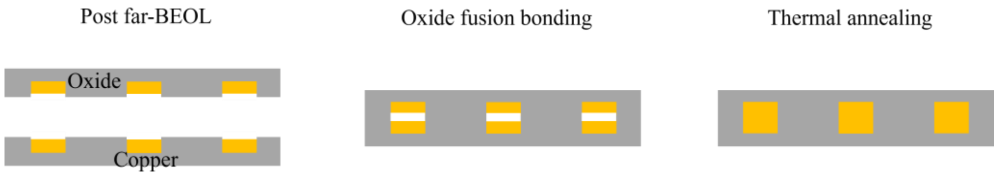

Fig. 2. A general process flow of hybrid bonding. It usually involves post-processed CMP surface on both surfaces before oxide fusion bonding and finally thermal annealing to form metal contacts.

The next question to address is how can two vertically separated optical interconnects coupled into each other? We had previously demonstrated free-space coupling between a pair of vertically coupled grating couplers in [8] and for inverted taper couplers, we found the answers in [9-11]. However, it remains unknown how efficient such vertical coupling can take place, considering that optical interconnects are usually embedded 6-8 µm underneath top oxide passivation for Si-PIC from foundries. Furthermore, far-back-end-of-line (far-BEOL) processing is needed to form the copper redistribution lines (RDL) and bond pads for hybrid bonding and will bury the optical interconnects further beneath the final oxide passivation, further increasing the gap between the pair of optical interconnects.

For the “passive” electronic-photonic interposer, it can be made of silicon or glass and come with through vias for electrical connectivity. The optical interconnects and waveguides on such interposers can be formed in the same way as they were formed on the Si-PIC but are buried less deep from the final oxide passivation layer. Glass interposers also have the additional freedom to form buried glass waveguides for mode expansion before optical interconnects and waveguides based on silicon or silicon nitride materials are deposited and patterned above them. Future work could be expanded to include free-space optics and for interposer pluggability either through external bonding such as [12] or using grayscale lithography to form the lenses directly on the interposer for out-of-plane coupling.

To first understand the coupling behavior of a pair vertically spaced grating coupler, we used the 340 nm SOI grating coupler design from [13] for simulation. Similarly, for the pair of silicon (Si) inverted tapers, we used 220 nm SOI and waveguide width of 450 nm. The waveguide was then linearly tapered through a length of 110 µm to end at a width of 120 nm. We also explored the coupling feasibility between a pair of silicon nitride (SiN) inverted tapers based on [14]. The SiN thickness was 400 nm with waveguide width of 840 nm. The waveguide was then linearly tapered through a length of 300 µm to end at a width of 150 nm. For all three optical interconnect structures, we first varied the vertical separation (z-position) and then explored the alignment tolerances (x- and y-positions) between them. We also compared the vertically coupled transmissions to a standard fibre coupling. The definitions of x-, y- and z-positions are shown in Fig. 1 earlier.

3. SIMULATION RESULT AND ANALYSIS

A. Pair of Grating Couplers

Fig. 3 shows the x-position tolerances of two vertically separated silicon grating couplers. x = 0 was referenced at the position where the last teeth of the bottom grating coupler met the first teeth of top grating coupler. We then scanned the top grating coupler in the negative direction and at various vertical separations (z-positions) to map the transmission passing from the bottom coupler to the top coupler. For the FDTD simulations, we used 2D setup for x-position scans to reduce computing resources and 3D setup for y-position scans. The simulation showed that transmission is relatively insensitive to the vertical gap (z-positions) and that the x-positions can be adjusted to optimize the transmission again. For example, at z = 2 µm, a peak transmission of 69.6% occurred at x = -17 µm while at z = 12 µm, a peak transmission of 72% occurred at x = -16 µm. The 1 dB tolerance for x-positions varied depending on the gap. For example, at z = 2 µm, the tolerance is approximately 6 µm while at z = 12 µm, the tolerance is approximately 5 µm. The 1 dB tolerance for y-positions on the other hand is approximately 8 µm at z = 12 µm (Fig. 4). Such 1 dB tolerances in the x- and y- positions are therefore sufficiently large for passive optical coupling during hybrid bonding, which can come with bonding accuracy of ~0.5 µm depending on equipment capability.

Lastly, we compared the bandwidth of regular fibre-to-grating couplers and a pair of vertically positioned grating couplers. We can see from Fig. 5 that the bandwidth of the latter is relatively broader than the former with a 1 dB tolerance of approximately 60 nm but has lower transmission efficiency. Nevertheless, we opined that grating coupler designs have further room for optimization and based on x- and y-tolerances, is a very attractive passive optical coupling approach for hybrid bonding integration.

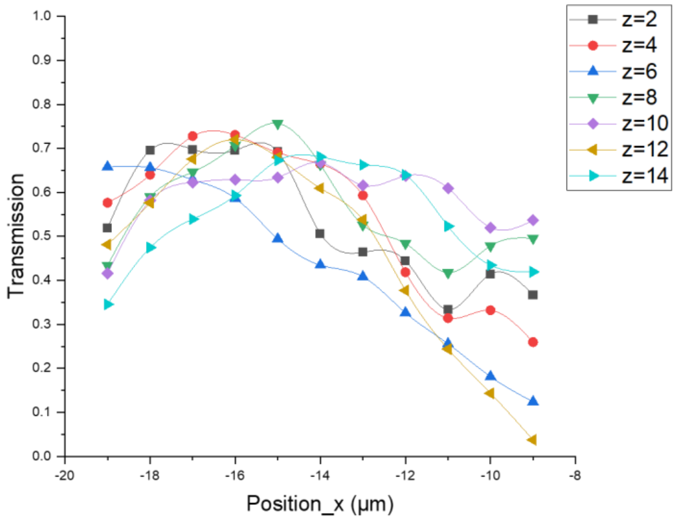

Fig. 3. 2D-FDTD transmission showing x-position tolerance of upper grating coupler relative to bottom grating coupler at various gaps (z-positions) while keeping y = 0. The 1 dB tolerance for x-positions varied depending on the gap.

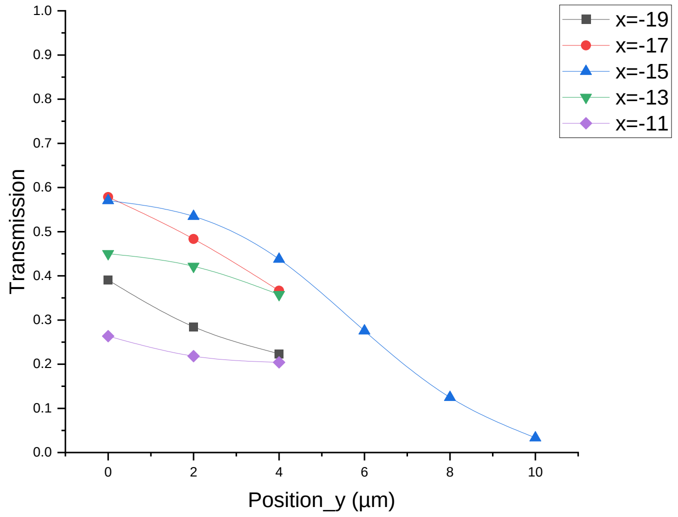

Fig. 4. 3D-FDTD transmission showing y-position tolerance of upper grating coupler relative to bottom grating coupler at various x-positions while keeping z = 12 µm. The 1 dB tolerance for y-positions is approximately 8 µm at x = -15 µm.

B. Pair of Inverted Tapers

Moving on to silicon inverted tapers, we can see from Fig. 6 that that transmission is very sensitive to vertical gaps (z-positions). Just like part A, we defined x = 0 at the tip of the taper and then scanned the top taper in the negative x-direction. For the FDTD simulations, we used 3D setup for both x-position and y-position scans. For x-position scans, we set the y-min boundary condition as anti-symmetric to reduce computing resources. From the simulations, we can see that at z = 0, a peak transmission of 94.7% occurred at x = -20 µm but dropped to 21.4% at z = 2 µm and dropped further to 1.4% at z = 4 µm. The results were not surprising as such evanescent coupling behavior had been previously documented and used in programmable MEMS photonics to achieve a high extinction ratio. Again, the 1 dB tolerance for x-positions varied depending on the gap. For example, at z = 1 µm, the tolerance is approximately 40 µm. We further explored the sensitivity of evanescent coupling between two inverted tapers in the y-direction and found that the tolerance is tighter at only 0.3 µm. This is to be expected as the waveguide width is only 0.45 µm, but we opined that the taper design can be optimized since we used common inverted taper meant for edge coupling in this activity. As for the bandwidth tolerances, we already knew that inverted tapers are broadband thus it was not meaningful to simulate them.

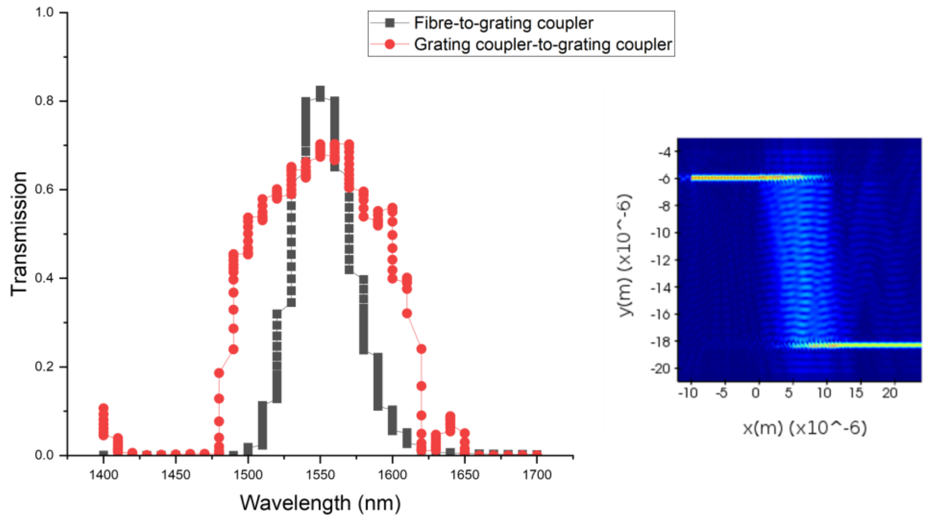

Fig. 5. 2D-FDTD transmission and bandwidth comparison between fibre coupling to grating coupler and a pair of grating coupler. The x- and y-positions of the pair of vertically separated grating coupler had been optimized at z = 12 µm. The 1 dB tolerance is approximately 60 nm. The figure on the right shows the electric field between the pair of grating couplers.

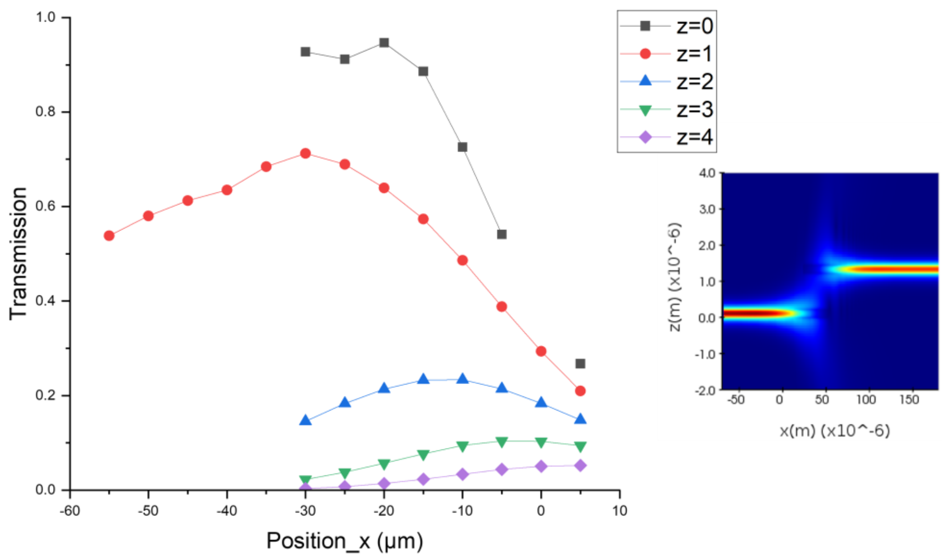

Fig. 6. 3D-FDTD comparison of x-position tolerance of upper silicon inverted taper relative to bottom silicon inverted taper at various z-position. Transmission between inverted tapers decreases as z increases. The figure on the right shows the electric field between the pair of inverted tapers at z = 1 µm and x = -30 µm.

Finally, for a pair of silicon nitride (SiN) inverted tapers (Fig. 7), we found that they allowed coupling at larger gap (z-position) compared to silicon inverted tapers, and this could be attributed to the larger mode field diameter compared to silicon inverted tapers. For instance, silicon inverted tapers had 39.4% peak transmission at z = 1.5 µm while SiN inverted tapers had 66.2% peak transmission at z = 1.6 µm. As z increases, transmission of silicon inverted tapers dropped to 11.1% at z = 2.5 µm but SiN inverted tapers still allow 31.9% transmission. Multi-layers of SiN inverted tapers can thus potentially be used to bring the embedded silicon inverted tapers buried underneath 6-8 µm of oxide passivation toward the surface for more efficient coupling during hybrid bonding.

4. CONCLUSION

We explored the feasibility of hybrid bonding between Si-PIC to optical interposer through FDTD simulations using two commonly used optical interconnects. We found that for a pair of grating couplers, transmission between them can occur even with thick oxide layer separating them in the z-direction, making them an attractive candidate for initial demonstration. On the other hand, transmission between a pair of silicon and silicon nitride inverted tapers are sensitive to gaps and drop drastically as the oxide layer separating them increases. The designs of such evanescently coupled inverted tapers is currently being studied and tuned to allow couplings with larger gaps.

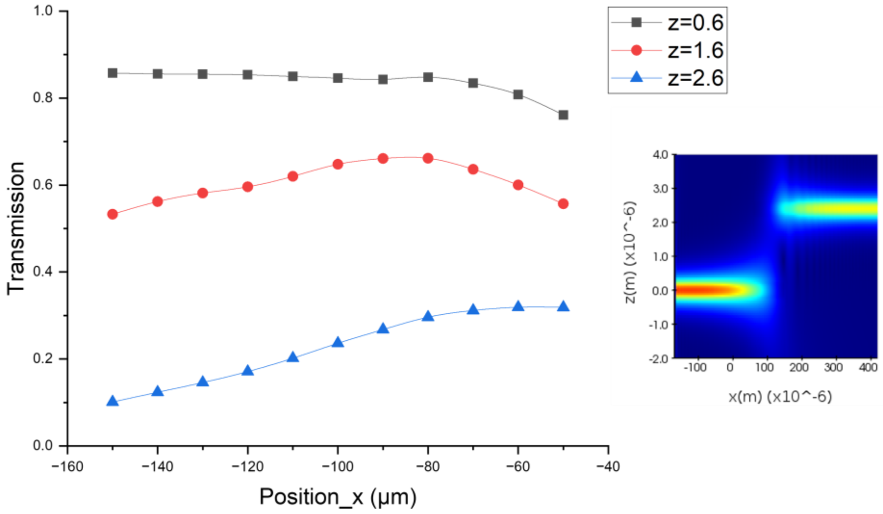

Fig. 7. 3D-FDTD comparison of x-position tolerance of upper silicon nitride inverted taper relative to bottom silicon nitride inverted taper at various z-position. Transmission between silicon nitride inverted tapers decreases as z increases, but less drastic than that of silicon inverted tapers. The figure on the right shows the electric field between the pair of inverted tapers at z = 1.6 µm and x = -90 µm

ACKNOWLEDGMENT

This activity has been supported by Science Foundation Ireland (SFI) under grant number 12/RC/2276 P2.

REFERENCES

1. A. Jouve *et al.*, "Die to Wafer Direct Hybid Bonding Demonstration with High Alignment Accuracy and Electrical Yields," *2019 International 3D Systems Integration Conference (3DIC)*, Sendai, Japan, 2019, pp. 1-7; doi: 10.1109/3DIC48104.2019.9058905.
2. J. Abdilla, "Die to Wafer Hybrid Bonding -The Next Generation of Advanced Packaging," *3D & Systems Summit*, 2022.
3. G. Gao et al., "Low Temperature Cu Interconnect with Chip to Wafer Hybrid Bonding," *2019 IEEE 69th Electronic Components and Technology Conference (ECTC)*, Las Vegas, NV, USA, 2019, pp. 628-635; doi: 10.1109/ECTC.2019.00100.
4. D. Liu, P.C. Chen, T.C. Chou, H.W. Hu, K.N. Chen, "Demonstration of Low-Temperature Fine-Pitch Cu/SiO2 Hybrid Bonding by Au Passivation," *Journal of the Electron Devices Society*, pp. 868-875, Vol. 9, 2021; doi: 10.1109/JEDS.2021.3114648.
5. V. Chidambaram, P. Lianto, X. Wang, G. See, N. Wiswell and M. Kawano, "Dielectric Materials Characterization for Hybrid Bonding," *2021 IEEE 71st Electronic Components and Technology Conference (ECTC)*, San Diego, CA, USA, 2021, pp. 426-431; doi: 10.1109/ECTC32696.2021.00078.
6. S. Yoneda et al., "Development of Polyimide Base Photosensitive Permanent Bonding Adhesive for Middle to Low Temperature Hybrid Bonding Processes," *2022 IEEE 72nd Electronic Components and Technology Conference (ECTC)*, San Diego, CA, USA, 2022, pp. 595-601; doi: 10.1109/ECTC51906.2022.00100.
7. M. Fowler, M. Dong, A. Guerrero, B. Huan, R. Puligadda, "A Novel Photosensitive Permanent Bonding Material Designed for Polymer/Metal Hybrid Bonding Applications," *CS Mantech Conference*, May 2022.
8. H. Y. Hwang et al., "Pluggable Silicon Photonic MEMS Switch Package for Data Centre," *2018 IEEE 20th Electronics Packaging Technology Conference (EPTC)*, Singapore, 2018, pp. 46-49; doi: 10.1109/EPTC.2018.8654270.
9. M. Passoni, F. Floris, H. Y. Hwang, L. Zagaglia, L. Carroll, L. C. Andreani, P. O'Brien, "Co-optimizing grating couplers for hybrid integration of InP and SOI photonic platforms," *AIP Advances*, 1 September 2018; 8 (9): 095109; doi: /10.1063/1.5046164.
10. Rong Sun, Mark Beals, Andrew Pomerene, Jing Cheng, Ching-yin Hong, Lionel Kimerling, and Jurgen Michel, "Impedance matching vertical optical waveguide couplers for dense high index contrast circuits," *Opt. Express 16*, 11682-11690 (2008).
11. Ryohei Takei, Yuriko Maegami, Emiko Omoda, Youichi Sakakibara, Masahiko Mori, and Toshihiro Kamei, "Low-loss and low wavelength-dependence vertical interlayer transition for 3D silicon photonics," *Opt. Express 23*, 18602-18610 (2015).
12. Saif Wakeel, Padraic E. Morrisey, Muhammet Genc, Prasanna Ramaswamy, Robert Bernson, Kamil Gradkowski, Brian Corbett, Peter O'Brien, "Micro-transfer printing of thick optical components using a tether free UV-curable approach," *J. Opt. Microsyst. 4(1)*, 011003 (2024); doi: 10.1117/1.JOM.4.1.011003.
13. L. Zagaglia, F. Floris and P. A. O'Brien, "Experimental Characterization of Particle Swarm Optimized Focusing Non-Uniform Grating Coupler for Multiple SOI Thicknesses," *Journal of Lightwave Technology*, vol. 39, no. 15, pp. 5028-5034, Aug.1, 2021; doi: 10.1109/JLT.2021.3079575.
14. B. Snyder et al., "Ultra-broadband, polarization-insensitive SMF-28 fiber edge couplers for silicon photonics," 2017 IEEE CPMT Symposium Japan (ICSJ), Kyoto, Japan, 2017, pp. 55-58, doi: 10.1109/ICSJ.2017.8240087.